Journal of Pharmaceutical Analysis 12 (2022) 424–435

Contents lists available at ScienceDirect

Journal of Pharmaceutical Analysis

journal homepage: www.elsevier.com/locate/jpa

Original article

# Compatibility and stability studies involving polymers used in fused deposition modeling 3D printing of medicines

Ihatanderson A. Silva [a], Ana Luiza Lima [a], Tais Gratieri [a], Guilherme M. Gelfuso [a], Livia L. Sa-Barreto [b], Marcilio Cunha-Filho [a, *]

[a] Laboratory of Food, Drug, and Cosmetics (LTMAC), School of Health Sciences, University of Brasilia, 70910-900, Brasília, DF, Brazil
[b] Faculty of Ceilandia, University of Brasilia (UnB), 72220-900, Brasília, DF, Brazil

ARTICLE INFO

*Article history:*
Received 23 May 2021
Received in revised form
3 September 2021
Accepted 17 September 2021
Available online 20 September 2021

*Keywords:*
Three-dimensional printing
Preformulation
Hot-melt extrusion
Thermal analysis
Drug-polymer compatibility

ABSTRACT

One of the challenges in developing three-dimensional printed medicines is related to their stability due to the manufacturing conditions involving high temperatures. This work proposed a new protocol for preformulation studies simulating thermal processing and aging of the printed medicines, tested regarding their morphology and thermal, crystallographic, and spectroscopic profiles. Generally, despite the strong drug-polymer interactions observed, the chemical stability of the model drugs was preserved under such conditions. In fact, in the metoprolol and Soluplus® composition, the drug's solubilization in the polymer produced a delay in the drug decomposition, suggesting a protective effect of the matrix. Paracetamol and polyvinyl alcohol mixture, in turn, showed unmistakable signs of thermal instability and chemical decomposition, in addition to physical changes. In the presented context, establishing protocols that simulate processing and storage conditions may be decisive for obtaining stable pharmaceutical dosage forms using three-dimensional printing technology.



## 1. Introduction

Preformulation is an important stage in drug product development, supporting medicines' manufacturing within quality and stability standards required for regulatory registration. Such study must be designed under tailored protocols to simulate the processes involved in pharmaceutical production, identifying possible deleterious interactions among the formulation components [1].

Several analytical tools can be used to characterize active pharmaceutical ingredients and excipients in preformulation studies [2]. Notably, derivative thermogravimetric analysis (DTG) and differential exploratory calorimetry (DSC) are advantageous in stimulating accelerated aging during the assay. By monitoring the enthalpy and mass loss involved in phase transition phenomena and chemical reactions, it is possible to access the sample stability under virtual processing and storage conditions [3]. In fact, the thermal analysis combined with spectroscopic and diffractometric measurements proves to be helpful in anticipating conclusions on drug stability in which the health guidelines of drug stability studies take several months to reach [4–7].

Recent studies show the outstanding potential of additive manufacturing in the pharmaceutical field [8–10], in which fused deposition modeling three-dimensional printing (3D/FDM) has been proven to be one of the most promising techniques to elaborate drug products [11]. Notably, a 3D-printed dosage form can have its composition, release kinetics, shape, and size specifically designed to meet patients' specific needs [12–14]. For this, the raw materials are initially subjected to pharmaceutical hot-melt extrusion (HME) to form drug-loaded filaments. Then, 3D/FDM printers build medicines under electronic control from these filaments' melting [15,16]. The filaments used in 3D/FDM printing are composed of plastic polymers heated in the print nozzle at temperatures above their glass transition and deposited in overlapping layers of variable height and dimension on a flat surface with heating control [17].

The avant-garde scenario of this recent technology, typical from the engineering of materials and brought to the

Peer review under responsibility of Xi'an Jiaotong University.
* Corresponding author.
*E-mail address:* marciliofarm@hotmail.com (M. Cunha-Filho).

https://doi.org/10.1016/j.jpha.2021.09.010

**Table 1**
Derivative thermogravimetric analysis (DTG) data for mass loss (%) occurring up to 350, together with differential exploratory calorimetry (DSC) results for melting peak (°C) and drugs crystallinity (%) of paracetamol (PCM) and metoprolol tartrate (MTL) as supplied and its binary mixtures untreated and subjected to longer aging time (90 days).

| Sample | DSC | | | | DTG | |
|---|---|---|---|---|---|---|
| | Melting peak (°C) | | Crystallinity (%) | | Mass loss (%) | |
| | Untreated | Aged 90 days | Untreated | Aged 90 days | Untreated | Aged 90 days |
| PCM | 171.2 | 170.9 | 100 | 91.1 | 100 | 100 |
| PCM-EUL | 170.2 | 171.8 | 62.8 | 77.7 | 43.4 | 45.3 |
| PCM-PVA | 166.1 | 169.8 | 100 | 79.4 | 98.6 | 80.8 |
| PCM-PVPVA | 170.1 | NA | 0.4 | 5.9 | 43.8 | 59.6 |
| PCM-SOL | 162.7 | 157.1 | 55.9 | 10.2 | 63.5 | 49.5 |
| MTL | 125.1 | 121.9 | 100 | 86.5 | 95.2 | 92.5 |
| MTL-EUL | 124.8 | 113.3 | 56.8 | 69.9 | 45.5 | 51.6 |
| MTL-PVA | 125.3 | 127.0 | 91.2 | 96.2 | 74.3 | 67.7 |
| MTL-PVPVA | 124.9 | 122.3 | 70.2 | 60.8 | 62.1 | 61.9 |
| MTL-SOL | 124.9 | 115.4 | 100 | 38.0 | 54.3 | 50.2 |

EUL: Eudragit® L100; PVA: Parteck® MXP; PVPVA: Plasdone®; SOL: Soluplus®; NA: not accessed.

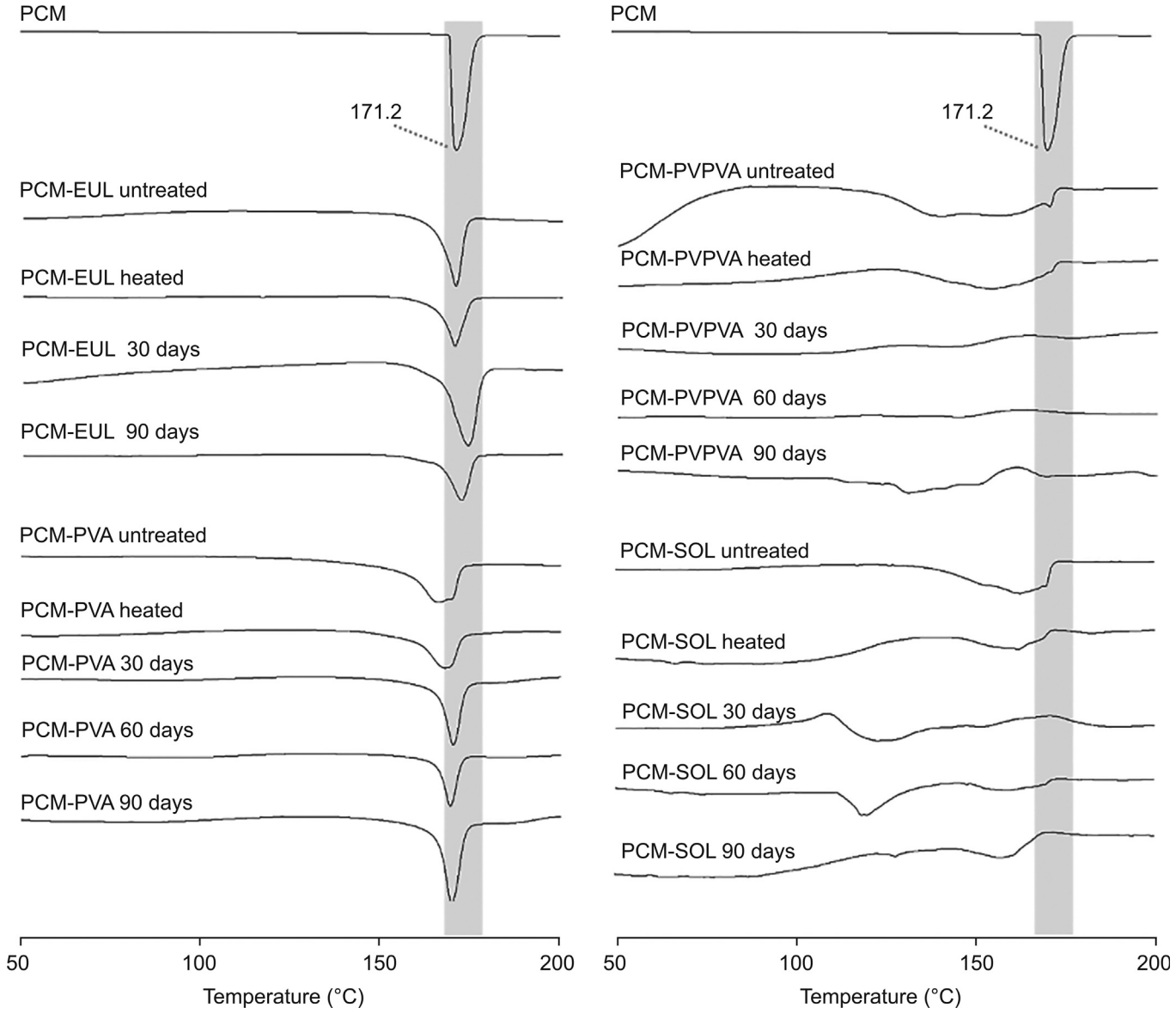


**Fig. 1.** Differential exploratory calorimetry (DSC) curves of paracetamol (PCM) as supplied and binary mixtures PCM-Eudragit® L100 (EUL), PCM-Parteck® MXP (PVA), PCM-Plasdone® (PVPVA), and PCM-Soluplus® (SOL) untreated and subjected to double heating (heated) and different aging time (30, 60, and 90 days). The PCM melting peak is shaded.

pharmaceutical field, brings potential risks to the product stability. Unlike the usual pharmaceutical manufacturing processes, such as granulation and compression, in which well-established preformulation protocols can simulate and make projections about the final product's stability, yet no procedures adapted to the new processes involved in the 3D printing of medicines were proposed. Furthermore, due to the recent incorporation of this technology in the pharmaceutical field, little is known about such printed products' stability, especially those containing thermo-sensitive drugs [18,19].

Thus, the present study aims to fill the gap between the preformulation of pharmaceutical dosage forms produced with HME and 3D/FDM printing by proposing a new protocol involving the simulation of the combined thermal stresses. To this end, four promising polymers for pharmaceutical use involving such technology were selected (Eudragit® L100 (EUL); Plasdone® (PVPVA); Parteck® MXP (PVA); and Soluplus® (SOL)), which were tested using two model drugs, paracetamol (PCM), as a thermoresistant drug; and metoprolol tartrate (MTL), as a thermosensitive drug. Drug-polymer sets were subjected to thermal stress, aged in a stability chamber, and evaluated regarding their morphology and thermal, crystallographic, and spectroscopic profiles.

## 2. Experimental

### 2.1. Materials

PCM (lot 1511337) was purchased by Purifarma (São Paulo, Brazil), and MTL (lot FN 81700006) was provided by Purifarma (Anápolis, Brazil). Plasdone® K-29/32 (poly (vinylpyrrolidone-co-vinyl acetate) (PVPVA), lot 002177615) was donated by Ashland Specialty Ingredients (Covington, LA, USA), Eudragit® L100 (EUL, methacrylic acid-methyl methacrylate copolymer, lot

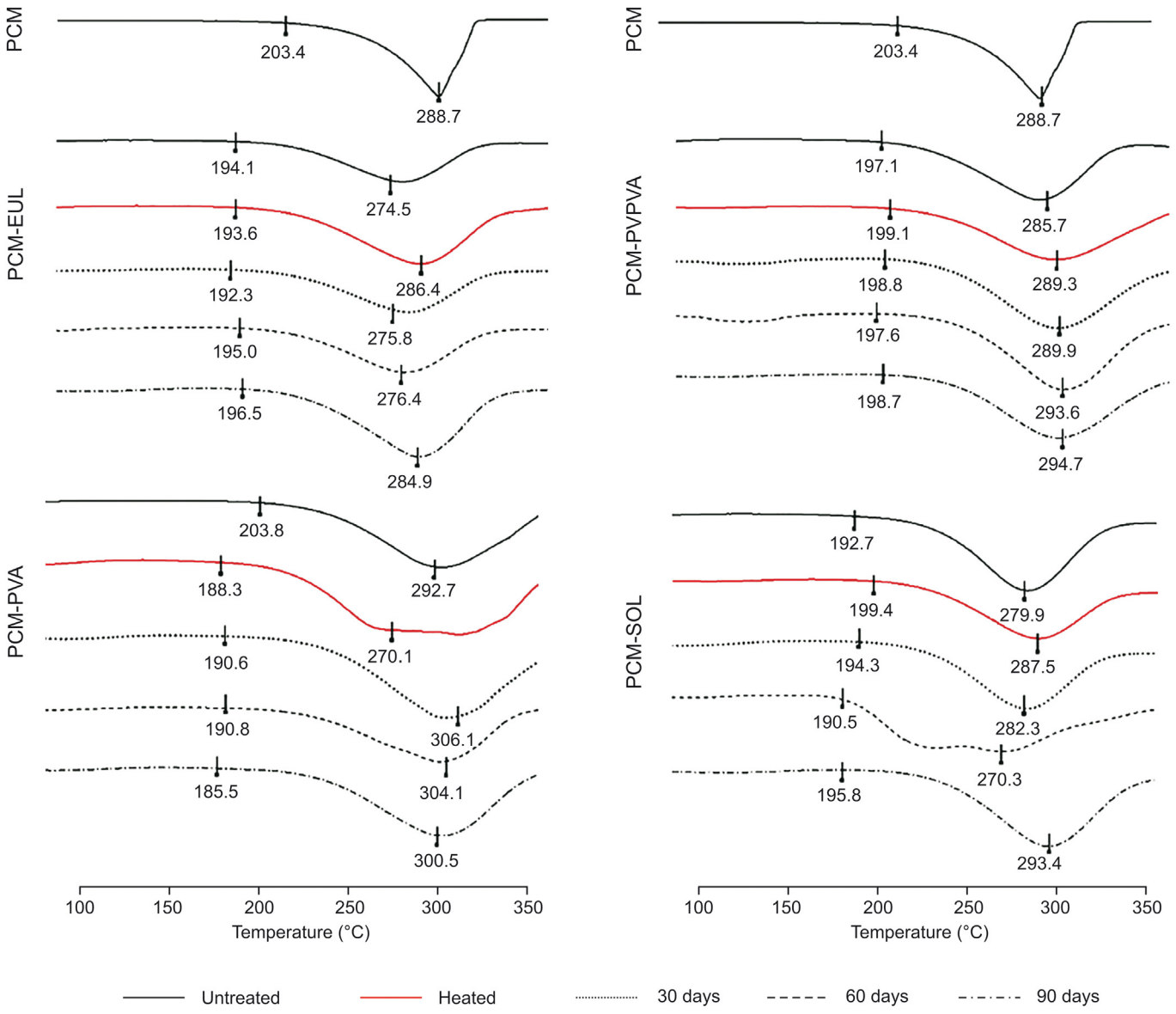


**Fig. 2.** Derivative thermogravimetric analysis (DTG) curves of PCM as supplied and binary mixtures PCM-EUL, PCM-PVA, PCM-PVPVA, and PCM-SOL untreated and subjected to double heating (heated) and different aging time (30, 60, and 90 days). The onset decomposition temperature and the temperature peaks of the decomposition phases are indicated.

B111003013) was provided by Evonik (Essen, Germany), Soluplus® (SOL, polyvinyl caprolactam-polyvinyl acetate-polyethylene glycol copolymer, lot 84414368E0) was a gift from BASF (Ludwigshafen, Germany), and Parteck® MXP (PVA, polyvinyl alcohol, lot F1952064) was donated by Merck (Darmstadt, Germany).

### 2.2. Sample preparation

To test the versatility of the proposed protocol, polymers with different physical-chemical properties, widely used in the pharmaceutical field and easy to adapt to the 3D printing of medicines, were selected. Remarkably, the pH-dependent solubility of EUL, the rapid aqueous disintegration of PVA, and the high hydrophilicity of SOL and PVPVA enable the preparation of different drug delivery systems by 3D-printing, such as gastro-resistant [20,21], immediate-release [22,23], and orodispersible [24] dosage forms.

Binary mixtures of each model drug (PCM or MTL) and a polymer (EUL, PVPVA, PVA, or SOL) in 1:1 (*m*/*m*) proportion were prepared and submitted to a double heating treatment, simulating the thermal stress of the manufacturing processes of HME and FDM/3D printing. Specifically, the samples (binary mixtures and their components alone) were heated twice in an oven for 2 min each, at temperatures commonly used for extrusion and printing based on the literature as follows: PVPVA mixtures (100 and 135 °C [25,26]); SOL mixtures (120 and 180 °C [27]); EUL mixtures (120 and 160 °C [28]); and PVA mixtures (160 and 180 °C [29,30]). The oven was equilibrated at each setpoint temperature before the samples were placed.

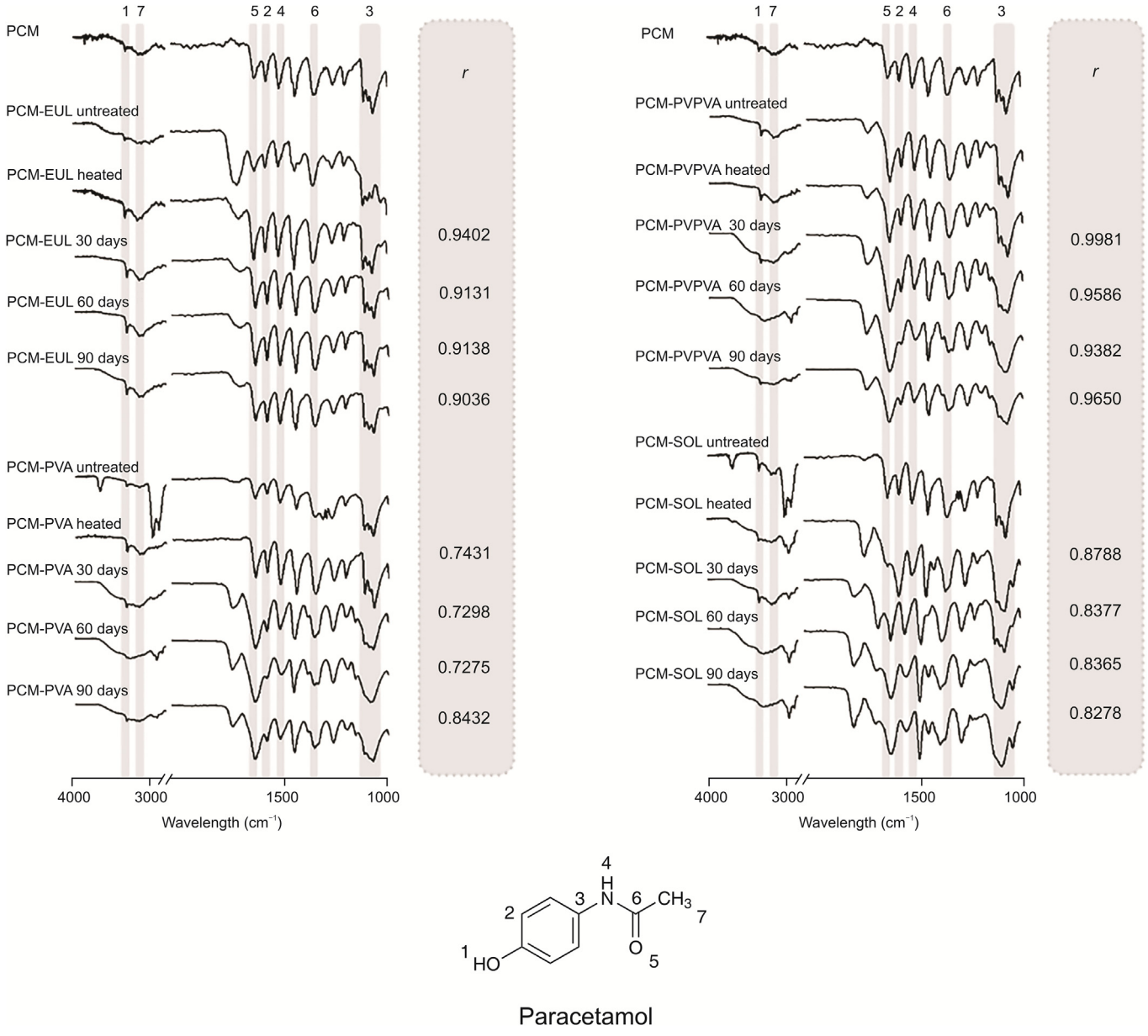


**Fig. 3.** Fourier transform infrared spectroscopy (FTIR) spectra of PCM as supplied and binary mixtures PCM-EUL, PCM-PVA, PCM-PVPVA, and PCM-SOL untreated and subjected to double heating (heated) and different aging time (30, 60, and 90 days). The bands related to the PCM functional groups are highlighted in the spectra and correlated with its chemical structure. The correlation coefficient (*r*) among the untreated and treated samples is also displayed.

Moreover, the samples were equilibrated at room temperature between the two heating processes.

Additionally, the double-heated samples were subjected to an accelerated stability protocol. Briefly, the samples in open containers were aged at 40 °C and 75% of relative humidity in a stability chamber (Nova Ética®, São Paulo, Brazil) for 3 months and analyzed at different time (15, 30, 60, and 90 days) according to the assays described as follows based on the FDA recommendations [4].

### 2.3. Thermal analysis

Thermal analysis tests were performed in the binary mixtures before and after double heating and accelerated aging at different time, as well as in the compounds alone subjected to the same treatments. Samples were evaluated by differential scanning calorimetry (DSC) performed in a previously calibrated DSC-60A equipment (Shimadzu®, Kyoto, Japan) using approximately 5 mg of the samples placed in aluminum crucibles. The equipment was operated under a dynamic $N_2$ atmosphere (50 mL/min) at 10 °C/min from 30 to 450 °C. The drug crystallinity in each mixture was calculated based on the drug melting enthalpy as supplied in percentage following the equation [31]:

$$\text{Drug crystallinity} = \Delta H_M / \Delta H_{drug} \times 100,$$

where $\Delta H_M$ is the drug melting enthalpy in the mixtures, and $\Delta H_{drug}$ is the melting enthalpy of the drug as supplied.

Thermogravimetric determinations were performed using approximately 5 mg of the samples placed in platinum crucibles under a 50 mL/min nitrogen flow using a Shimadzu DTG-60H (Kyoto, Japan). The equipment was operated at 10 °C/min in the range of 30–450 °C. Thermal data were processed by the TA software version 2.21 (Shimadzu, Kyoto, Japan) and plotted with the OriginPro software version 9.65 (Originlab Corp., Northampton, MA, USA).

### 2.4. X-ray powder diffraction (XRPD)

XRPD spectra were obtained in a Bruker D8 Discover (Karlsruhe, Germany) for untreated and "aged-90 days" samples. For this analysis, the diffraction patterns were obtained on angles in the range of 5° to 60° (2θ) in scan speed of 2°/min and step size of 0.02°.

### 2.5. Fourier transform infrared spectroscopy (FTIR)

Infrared spectra of binary mixtures and their components alone (untreated, double heated, and aged) were recorded in a transmittance range from 600 to 4000 $cm^{-1}$ (optical resolution of 4 $cm^{-1}$) in a Varian 640 FTIR spectrometer (Agilent Technologies, Santa Clara, CA, USA). Comparisons among untreated and treated samples were performed; the correlation coefficient was calculated using the Essential FTIR software version 3.50 (Operant LLC, Burke, VA, USA) [7].

### 2.6. Microphotographs

The morphological aspect of the samples (untreated, double heated, and aged) was analyzed by optical microscopy using a stereoscope connected to a video camera (Laborana/SZT, São Paulo, Brazil). The images were plotted using the Microsoft Windows Paint software version 4.1, and no masks or filters were applied to the original pictures.

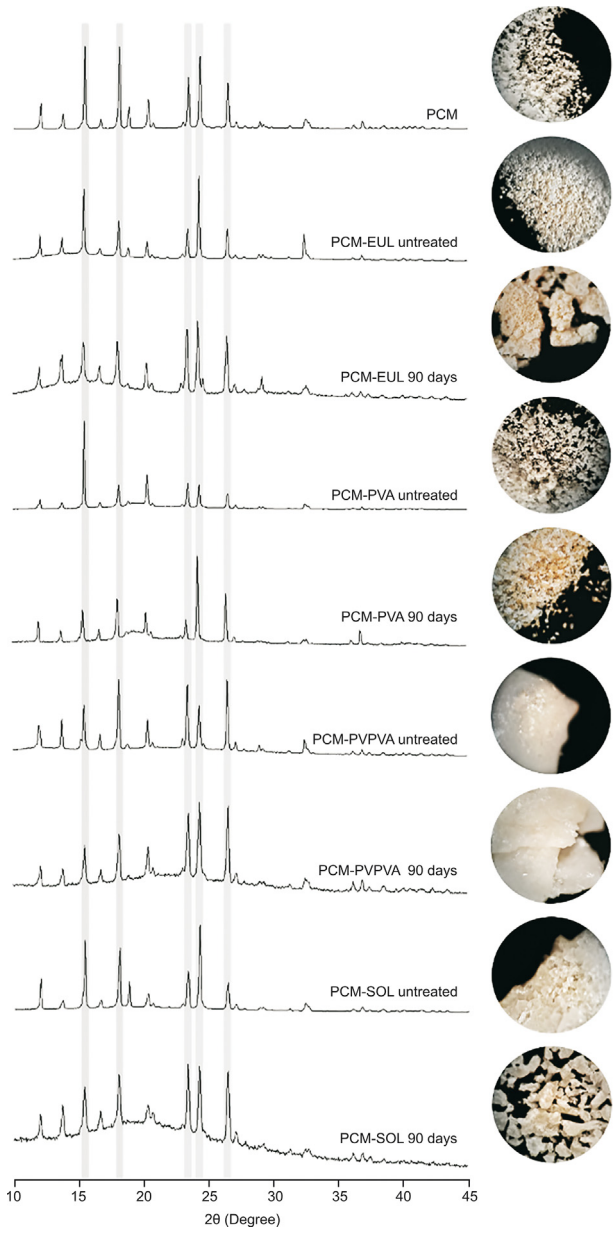


**Fig. 4.** X-ray powder diffraction (XRPD) diffractograms and optical micrographs of PCM as supplied and binary mixtures PCM-EUL, PCM-PVA, PCM-PVPVA, and PCM-SOL untreated and aged. The characteristic peaks of crystal PCM are shaded in diffractograms (15.45°, 18.15°, 23.45°, 24.35°, and 26.50°). The photomicrography magnification was ×4.5.

## 3. Results and discussion

### 3.1. Thermal processing of the selected model drugs

HME and 3D printing processes involve temperatures much higher than those required in the traditional pharmaceutical production of solid dosage forms, even considering operations that also demand heating, such as drying or granulation. Moreover, even temperatures considered low for HME/FDM processing are conditions of high thermal stress for pharmaceutical systems [32]. Despite the speed involved in the HME and 3D printing, which take only a few minutes to be performed, in both processes, temperatures above 100 °C are required, which can

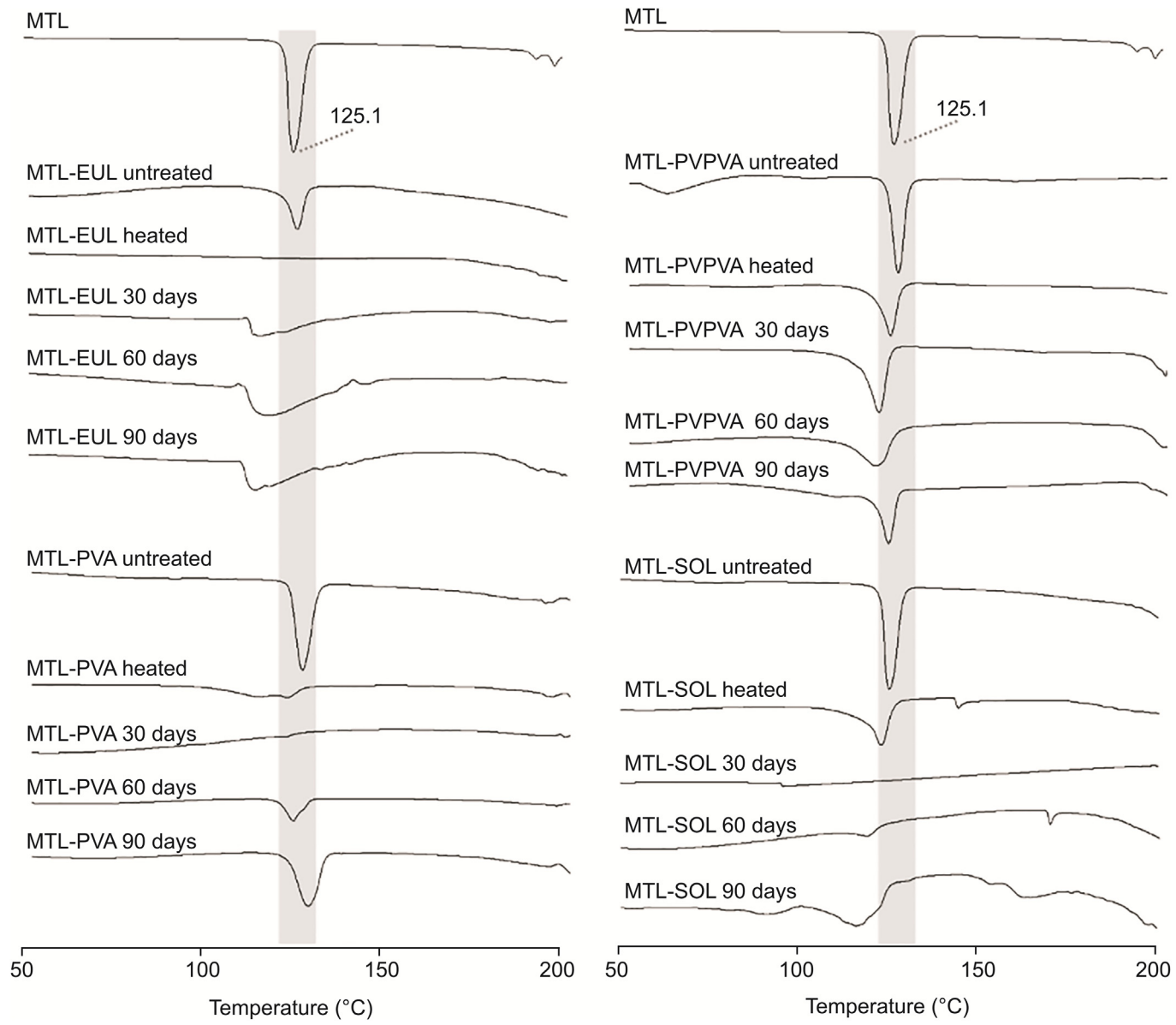


**Fig. 5.** DSC curves of metoprolol tartrate (MTL) as supplied and binary mixtures MTL-EUL, MTL-PVA, MTL-PVPVA, and MTL-SOL untreated and subjected to double heating (heated) and different aging time (30, 60, and 90 days). The MTL melting peak is shaded.

affect the stability of the dosage form, entailing a non-desirable degradation [15,18]. Therefore, the study's protocol was designed to investigate physicochemical repercussions on selected model drugs' stability when inserted in polymeric matrices under heating and aging.

PCM was chosen as a thermostable drug because it has also been used as a model in several other studies [33–35]. In fact, according to the DTG analyses, the decomposition of this drug occurred in one step at high temperatures in the range of 200–305 °C (Table 1). The heating used in this study to simulate HME processing and 3D printing was in the range of 160–180 °C, which was relatively out of the drug decomposition interval. The DSC profile of the PCM alone submitted to double heating and subsequently aged in a climatic chamber showed these treatments practically did not cause changes in the drug's melting event, which remained in the same temperature range ($T_{peak}$ around 171 °C). The PCM decomposition profile did not change either, even after 90 days of aging, with a $T_{peak}$ of DTG at 295 °C.

The FTIR bands of the PCM functional groups were also preserved in all conditions analyzed (Fig. S1). The correlation coefficients between the spectra of the untreated drug and the treated samples showed values between 0.90 and 0.93, confirming the preservation of the drug's chemical stability under such conditions. Nevertheless, the samples' heating was enough to stimulate drug melting and subsequent recrystallization without altering the drug's crystalline phase, as demonstrated by the X-ray diffraction spectra (Fig. S2A).

MTL, in turn, was chosen as a thermosensitive model drug [36–38]. Indeed, the DTG showed an intense mass loss in the range of 170–240 °C. Unlike PCM, the heating used to simulate the extrusion and printing processes (160 and 180 °C, respectively)

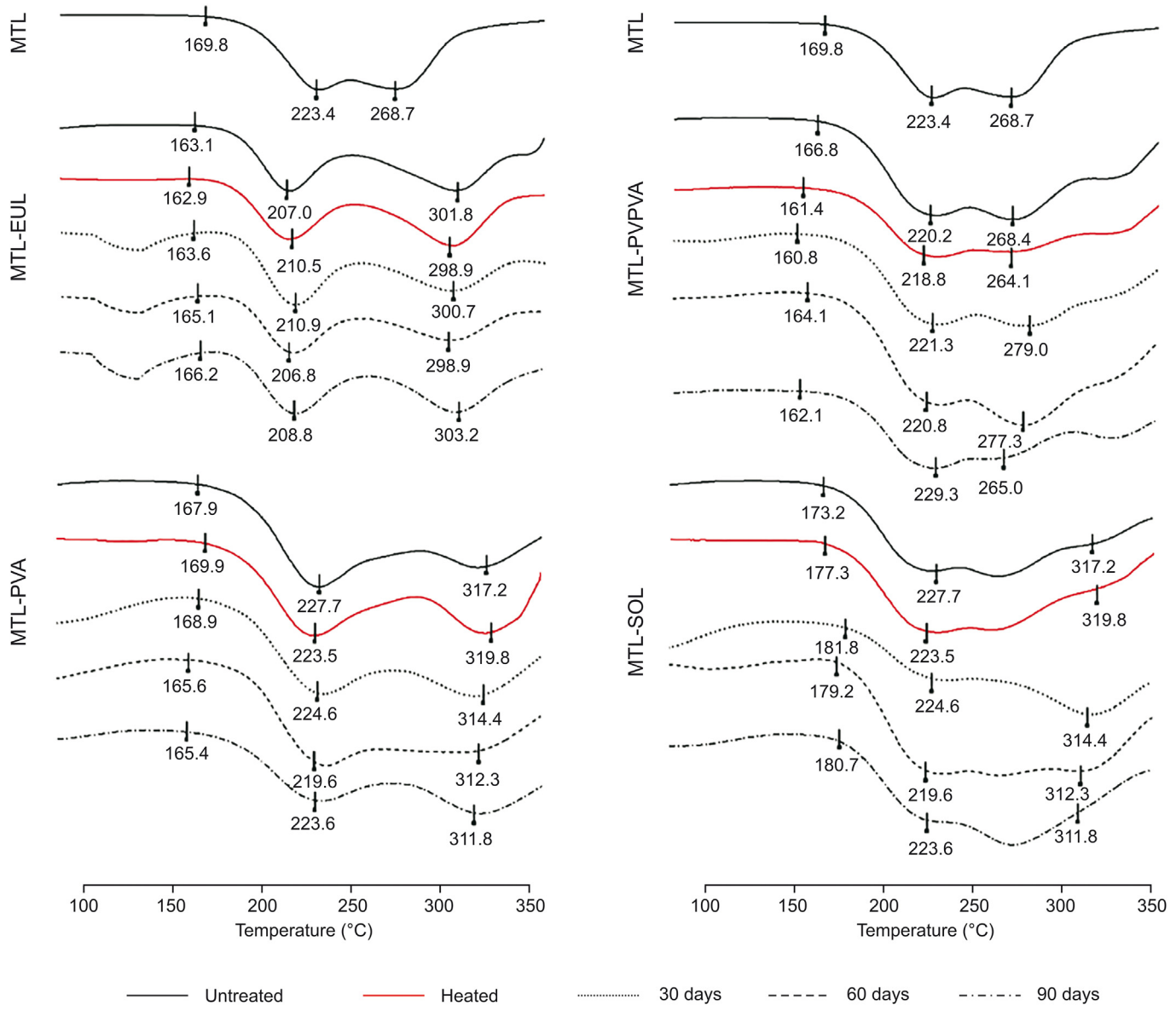


**Fig. 6.** DTG curves of metoprolol tartrate (MTL) as supplied and binary mixtures MTL-EUL, MTL-PVA, MTL-PVPVA, and MTL-SOL untreated and subjected to double heating (heated) and different aging time (30, 60, and 90 days). The onset decomposition temperature and the temperature peaks of the decomposition phases are indicated.

involves temperatures that could trigger the drug's chemical decomposition. The DSC of the double heated and aged samples showed a shift of the drug melting to lower temperatures, more markedly over time, reaching a change of 4 °C in the case of MTL aged-90 days, with a reduction of about 15% in its enthalpy (Table 1).

Despite this, the FTIR spectra of the MTL samples submitted to accelerated aging showed a high correlation coefficient with those of the untreated sample (above 0.9), evidencing that although the drug chemical decomposition is a possibility, as suggested by the thermal data, such a deleterious process is only initial and does not compromise the sample to a great extent. Indeed, the main drug FTIR bands were all recognized in MTL aged-90 days (Fig. S3). Also, the drug crystals had the same original crystalline phase, with a minor oscillation of the baseline, indicating traces of the amorphous drug in the sample (Fig. S2B).

### *3.2. Thermal processing and aging of the polymeric matrices with PCM*

Due to successive HME and 3D/FDM printing, thermal stress may increase the risk of possible harmful interactions between the drug and the excipients used to produce 3D-printed medicines [18]. Unlike capsules and tablets, in such modern medicines, a more intrinsic contact is established between the formula components, i.e., the drug is embedded in the polymer, creating intermolecular interactions such as van der Waals forces and hydrogen bonds. In this sense, the development of adapted protocols to verify drug-excipient compatibility is of even greater importance in guaranteeing drug products' stability.

The incorporation of PCM into EUL did not change the thermal profile of the drug. Indeed, both the melting event and the typical decomposition profile of PCM appeared practically unaffected even after the accelerated aging of the samples (Figs. 1 and 2). The

infrared spectra corroborated these findings, showing all the bands corresponding to the drug functional groups, with a high correlation coefficient (above 0.9) of the fresh sample compared to the treated and/or aged samples (Fig. 3). It endorsed the chemical compatibility between these components in such processing conditions.

Still, the results of XRPD showed the maintenance of the original crystalline phase of PCM, which presented the prominent diffraction peaks at 15.5°, 18.2°, 23.5°, 24.4°, and 26.5° (2θ) (Fig. 4). However, an increased amorphous component was observed in the PCM-EUL "aged-90 days" sample, suggesting the aging may have stimulated interaction among the mixture components, leading to partial solubilization of the drug in the polymer, which was corroborated by a drug crystallinity of 62.8%, as calculated by DSC (Table 1). A similar effect has recently been reported in matrix tablets of acrylic polymers containing PCM [39]. The literature shows that EUL has a high affinity for PCM by establishing hydrogen bonds with this drug's amide group [40]. Optical microscopy images corroborated this hypothesis by showing the formation of slightly yellow agglomerates (Fig. 4).

PCM-PVPVA mixtures, on the other hand, showed substantial thermal changes in the DSC (Fig. 1). Notably, the peak of drug melting completely disappeared, even in the untreated samples, indicating a strong drug-polymer thermal interaction. In contrast, XRPD diffractograms revealed that the drug had a crystalline profile in samples with PVPVA (Fig. 4) and DTG data indicated that the drug's decomposition profile did not reveal changes, with its decomposition intervals in agreement with the PCM alone (Fig. 2).

These findings indicate that the intense thermal interaction between these components observed by DSC was due to the solubilization of the drug in the polymer matrix during this analysis since it is possible to identify PCM diffraction peaks in the binary mixture. In fact, the infrared spectra showed that the bands corresponding to the PCM's functional groups could be identified without modifications, with a great correlation between the spectra of the untreated mixtures and stressed samples ($r > 0.95$). The smoothing of the band at 1258–1224 $cm^{-1}$ corresponding to C–N stretching may be related to the drug solubilization in the polymer and the formation of hydrogen bonds (Fig. 3).

The aging of the PCM-PVPVA under high relative humidity conditions caused a visible water uptake and agglomerates' formation (Fig. 4), however, without causing damage to the sample's chemical stability. This polymeric matrix's hygroscopicity is reported in other studies [29,41], suggesting the storage of printed medicines based on this polymer should be placed using impermeable packaging. Also, the PCM's diffractometric profile could be recognized in samples with a maximum level of aging (Fig. 4). Still, an increased amorphous component was noted regarding the drug's solubilization in PVPVA, as suggested by the DSC profile. Thus, the PCM was compatible with PVPVA even in extreme temperature conditions, such as a previously reported study for the physical mixture of these components without involving simulated conditions of double heating and aging [42].

Different from the two pairs of drug-polymer mentioned to this point, in which the thermo-resistant model drug was compatible with the polymeric vehicles EUL and PVPVA despite the thermal stress and accelerated aging, a different outcome was observed for the mixture containing PVA. The DSC profile presented in Fig. 1 showed that in the untreated sample, there was an anticipation of drug melting at approximately 5 °C, indicating an interaction between them. Such thermal interaction seemed to decrease with

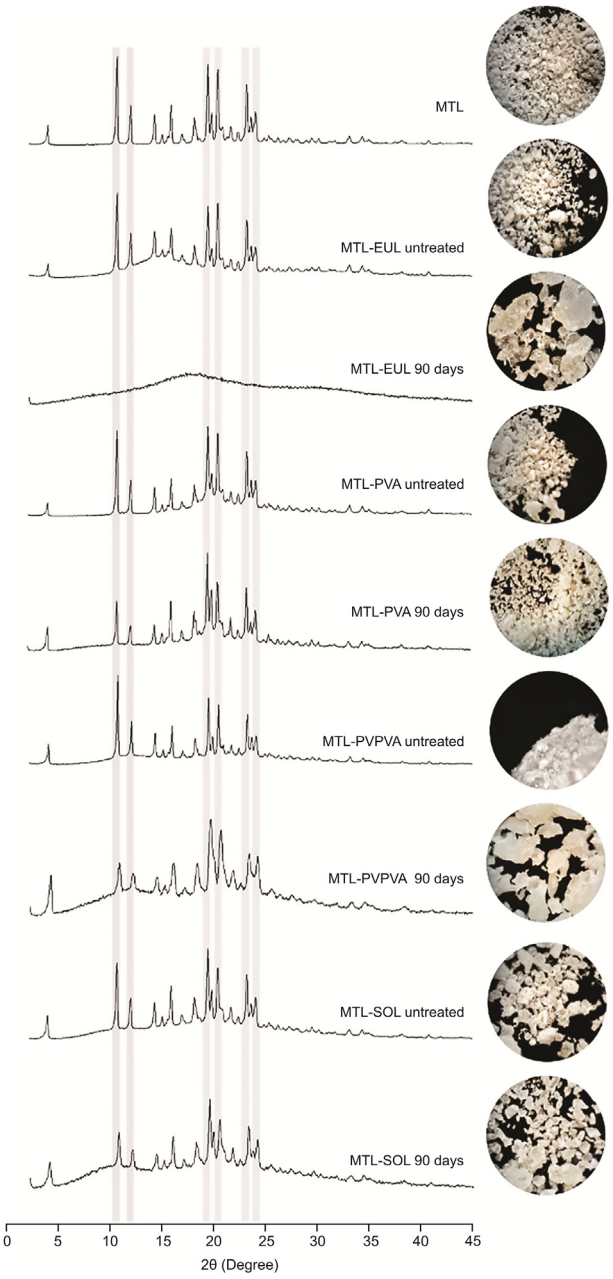


**Fig. 7.** XRPD diffractograms and optical micrographs of MTL as supplied and binary mixtures MTL-EUL, MTL-PVA, MTL-PVPVA, and MTL-SOL untreated and aged. The characteristic peaks of crystal MTL are shaded in diffractograms (10.55°, 11.85°, 19.35°, 20.30°, 23.10°, and 23.95°). The photomicrography magnification was ×4.5.

the samples' aging, which exhibited less intense changes in the drug melting.

In turn, DTG showed that while the decomposition profile of PCM was recognized in the untreated PCM-PVA with $T_{onset}$ at 203 °C (Fig. 2), the sample that underwent double heating revealed a change in the degradation profile, which included the anticipation of decomposition by about 15 °C. This stability loss was accentuated in the PCM-PVA "aged-90 days", whose decomposition started at 185 °C, even before the end of the drug melting event.

The FTIR spectra of these samples plotted in Fig. 3 revealed intensity loss of the bands corresponding to the drug's functional groups, especially in the bands at 1609 and 1562 $cm^{-1}$, corresponding

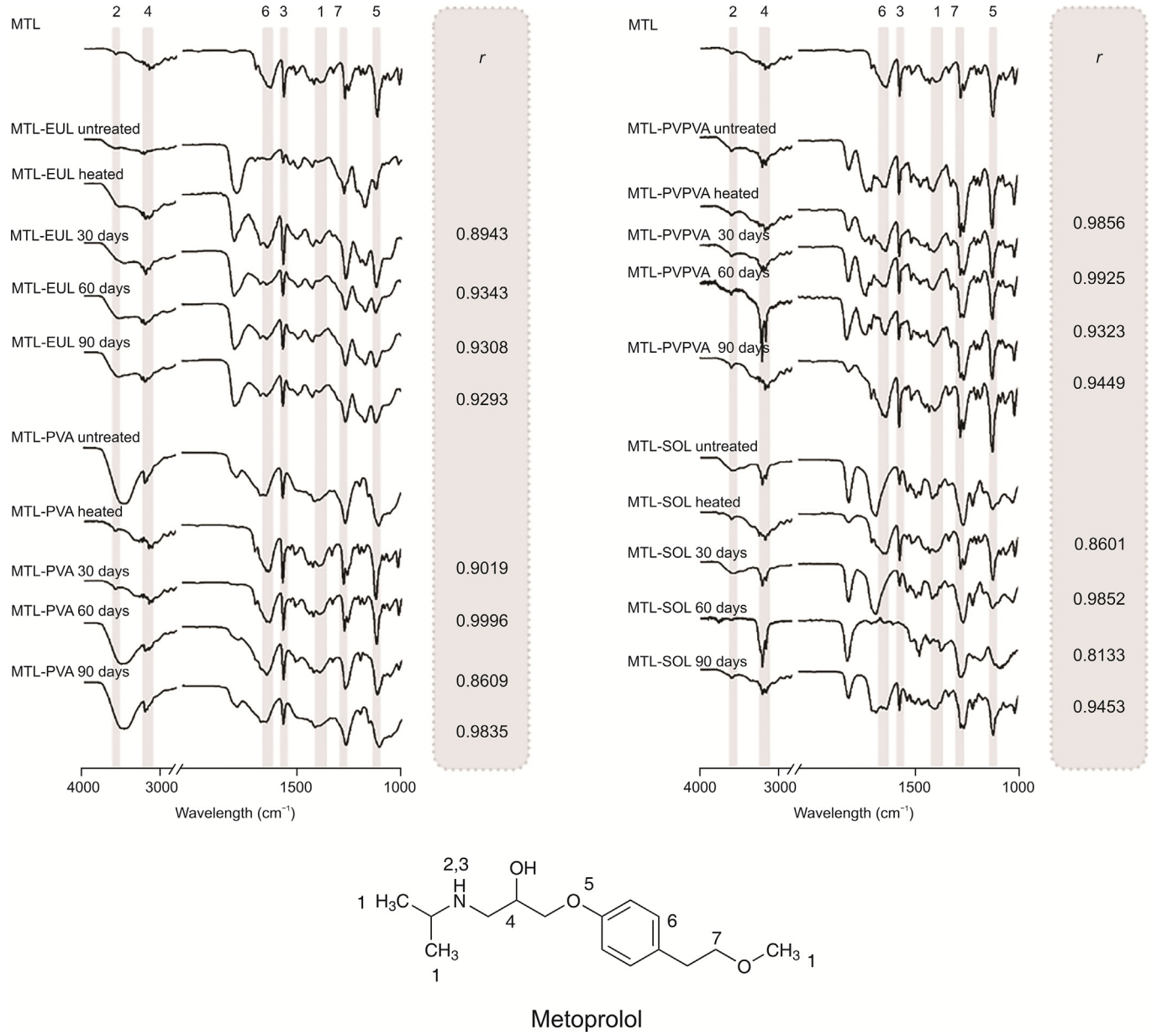


**Fig. 8.** FTIR spectra of MTL as supplied and binary mixtures MTL-EUL, MTL-PVA, MTL-PVPVA, and MTL-SOL untreated and subjected to double heating (heated) and different aging time (30, 60, and 90 days). The bands related to the PCM functional groups are highlighted in the spectra and correlated with its chemical structure. The correlation coefficient (*r*) among the untreated and treated samples is also displayed.

to the aromatic C=C stretching and N–H bending, respectively. Also, the band at 1258–1224 $cm^{-1}$ corresponding to the C–N stretching lost definition. Consequently, these samples' correlation coefficients presented reduced values (in the range of 0.7–0.8).

Such findings together suggest chemical reactions involving the drug. Moreover, the morphology of the sample PCM-PVA "aged-90 days" revealed a marked darkening of the powder, showing brownish crystals (Fig. 4). This is also observed as oscillations in the X-ray diffractogram baseline, especially in the range of 17° and 23° (2θ), suggesting an amorphous profile of the degradation products arising from the chemical reactions between the components (Fig. 4).

In this combination of PCM and PVA, the double heating to simulate extrusion and 3D printing processes highlighted the tendency to deleterious chemical reactions between the drug and the polymer, making clear the chemical incompatibility under customary conditions of pharmaceutical production had not been observed yet. In fact, this polymer was used in different pharmaceutical systems containing PCMs such as pellets, nanoparticles, and microemulsions, without showing signs of incompatibility [43–45].

Finally, SOL showed a strong affinity for PCM according to the DSC profiles exhibited in Fig. 1. While in the untreated mixture, the drug melting appeared quite wide; this event disappeared after the double heating, suggesting the complete solubilization of the drug in the polymeric matrix after the thermal treatment. Moreover, the mass loss profile of these samples occurred in the same temperature range, with minor oscillations, according to the DTG data (Fig. 2). We also observed small changes in the PCM characteristic bands (Fig. 3), which might be caused by establishing interactions

with the polymer, such as hydrogen bonds, particularly in the band at 1649 $cm^{-1}$ related to the drug carbonyl group [26]. The sample with the maximum degree of aging (PCM-SOL "aged-90 days") preserved the drug's crystalline profile, although it quite attenuated due to the high drug-polymer interaction observed in this sample (Fig. 4). Still, the sample's morphology revealed aggregates' formation without any color change, corroborating the chemical stability of this mixture.

### 3.3. Thermal processing and aging of the polymeric matrices with MTL

The mixture MTL-EUL showed a strong thermal interaction between the components after the double heating, with the disappearance of the melting event in the DSC curve of this sample, indicating complete solubilization of the drug in the polymeric matrix after such thermal processing (Fig. 5). In aged samples, a small crystallization of the drug could be seen involving reduced enthalpy. Even so, the thermal decomposition profile of MTL could be recognized in all evaluated samples (Fig. 6). Notably, the $T_{onset}$ involving the first stage of mass loss by decomposition at 169 °C showed oscillations of only a few degrees even after forced aging. Interestingly, this formulation's aging caused an unexpected water uptake in the sample, up to 7% in MTL-EUL "aged-90 days".

The predominantly amorphous diffractometric profile of the MTL-EUL in the aged-90 days sample confirmed the drug remained mostly dissolved in the polymeric matrix even after forced aging. As observed by optical microscopy, the glassy morphology of this sample corroborated this conclusion (Fig. 7). The hygroscopicity of MTL was possibly accentuated in its amorphous form, which explains the uptake of water under conditions of high relative humidity storage [46].

Even so, based on FTIR results, it is possible to reject the sample decomposition since the functional groups of the drug are preserved in the spectra, including the sample with the highest degree of aging (MTL-EUL "aged-90 days"). Furthermore, the correlation coefficients of the untreated sample's spectrum and the aged samples' spectra showed values consistently above 0.9 (Fig. 8), thus corroborating the drug-polymer compatibility. Similar findings have been found in matrix MTL mixtures containing different acrylic polymers produced using heating [47,48].

In the mixture containing MTL and PVPVA that underwent double heating, a slight broadening of the melting peak was observed, with an anticipation of 2–6 °C. This thermal interaction is accentuated with the sample aging, possibly due to the plasticizing effect of this polymer's water uptake [29]. The DTG curves suggest this association did not impair the drug's stability since the first decomposition mass loss event occurred in the same temperature range as the MTL alone (Fig. 6). Additionally, the samples' infrared spectra did not show changes in the bands of the drug's functional groups, showing a high correlation with the untreated sample (Fig. 8). The vitreous aspect and strong amorphous component in the sample based on the XRPD spectra confirm the partial drug solubilization in the polymeric matrix (Fig. 7).

The MTL samples mixed with PVA or SOL showed signs of strong drug-polymer interaction with the almost disappearance of the drug melting event, suggesting drug solubilization in the polymeric matrices after the double heating that simulated the extrusion and 3D printing processes (Fig. 5). The microscopical appearance of the aged samples was glassy and had no color changes. Also, their diffractometric profile had a crystalline component that coincided with the initial crystalline phase of the MTL, presenting the main diffraction peaks at 10.6°, 11.9°, 19.4°, 20.3°, 23.1°, and 24.0° (2θ) (Fig. 7). However, there is still a strong amorphous component in the mixture, corroborating the DSC findings.

In the composition containing MTL and PVA, the decomposition profile obtained by DTG was compatible with what was observed for the drug alone (Fig. 6). In contrast to PCM-PVA, there was no morphological or color change in aged MTL-PVA samples (Fig. 7). The infrared spectra showed only oscillations of bands, which can be attributed to the interactions established by the components due to the solubilization of the drug in the polymeric matrix, confirming their chemical compatibility with each other (Fig. 8).

In the mixture containing MTL and SOL, the interaction between the components changed the mixture's decomposition profile, whose temperature range occurred at least 10° later than expected, suggesting a protective effect of the polymer matrix. Moreover, in some samples of this mixture, we observed attenuation and displacement of infrared bands, particularly those bands at 3455 and 1512 $cm^{-1}$ corresponding to stretching and bending of NH group, respectively, which can be attributed to the formation of hydrogen bonds. The sample with the longest aging time (MTL-SOL "aged-90 days") showed a high correlation with the untreated mixture in the FTIR spectra, proving the chemical integrity of MTL, despite the strong drug-polymer interaction which, in this case, produced positive consequences for the stability of the system. Similar results were achieved with SOL-HME systems loading carbamazepine and itraconazole [49,50].

Thus, the preformulation protocol used in this study allowed to simulate the thermal stresses involved in the HME and 3D/FDM printing processes rapidly and straightforwardly with reliable results, using analytical tools accessible to the routine of pharmaceutical production.

## 4. Conclusions

This study, involving two model drugs with different sensitivity to temperature and four polymeric matrices, showed despite the thermal stress accumulated in the double thermal processing of the samples and their forced aging, there are good prospects that these drug products have adequate stability for commercialization.

Even in certain circumstances, interactions with polymers act as a protective factor to the drug, as observed between the thermosensitive drug MTL and SOL. In contrast, drug-excipient incompatibilities that can go unnoticed in conventional solid dosage forms can negatively affect 3D printing medicines due to thermal inheritance and the close relationship between the formulation's components as observed in the association of PCM and PVA. In this context, establishing protocols that simulate processing and storage conditions proposed in this work can be decisive for obtaining stable pharmaceutical dosage forms using this new technology.

## CRediT author statement

**Ihatanderson A. Silva:** Methodology, Formal analysis, Investigation, Data curation, Writing - Original draft preparation; **Ana Luiza Lima:** Data curation, Validation, Writing - Reviewing and Editing; **Tais Gratieri:** Formal analysis, Resources, Writing - Reviewing and Editing; **Guilherme M. Gelfuso:** Validation, Formal analysis, Investigation, Writing - Reviewing and Editing; **Livia L. Sa-Barreto:** Conceptualization, Formal analysis, Resources; **Marcilio Cunha-Filho:** Conceptualization, Formal

analysis, Investigation, Resources, Supervision, Writing - Reviewing and Editing.

## Declaration of competing interest

The authors declare that there are no conflicts of interest.

## Acknowledgments

This research was financially supported by the Brazilian agencies DPI/UnB, FAP-DF (Grant No.: 193.001.741/2017), and CNPq (Grant No.: 408291/2018–4). The authors would like to thank the contribution of Ms. Daniela Galter and Ms. Karina Riccomini from Ashland Specialty Ingredients, Ms. Beatriz Pancica from Merck, Ms. Renata Colenci from Evonik, and Mr. Fabio Ito from BASF for kindly supplying the material used in this work. Additionally, the authors thank the laboratory LaProNat/UnB for allowing the use of its facilities.

## Appendix A. Supplementary data

Supplementary data to this article can be found online at https://doi.org/10.1016/j.jpha.2021.09.010.

## References

[1] I. Alves-Silva, L.C.L. Sá-Barreto, E.M. Lima, et al., Preformulation studies of itraconazole associated with benznidazole and pharmaceutical excipients, Thermochim. Acta 575 (2014) 29–33.
[2] M.K. Trivedi, N. Dixit, P. Panda, et al., In-depth investigation on physicochemical and thermal properties of magnesium (II) gluconate using spectroscopic and thermoanalytical techniques, J. Pharm. Anal. 7 (2017) 332–337.
[3] A. Talvani, M.T. Bahia, L.C.L. de Sá-Barreto, et al., Carvedilol: Decomposition kinetics and compatibility with pharmaceutical excipients, J. Therm. Anal. Calorim. 115 (2014) 2501–2506.
[4] Food and Drug Administration, Pharmaceutical Development Report Example QbD for IR Generic Drugs, 2012. Module 3 Quality 3.2.P.2 Pharmaceutical Development. https://www.fda.gov/files/drugs/published/quality-by-design-%28QbD%29-for-an-immediate-release.pdf. (Accessed 14 July 2021).
[5] R. Ferreira-Nunes, T. Gratieri, G.M. Gelfuso, et al., Mixture design applied in compatibility studies of catechin and lipid compounds, J. Pharm. Biomed. Anal. 149 (2018) 612–617.
[6] B. Rojek, B. Suchacz, M. Wesolowski, Artificial neural networks as a supporting tool for compatibility study based on thermogravimetric data, Thermochim. Acta 659 (2018) 222–231.
[7] F.Q. Pires, L.A. Pinho, D.O. Freire, et al., Thermal analysis used to guide the production of thymol and *Lippia origanoides* essential oil inclusion complexes with cyclodextrin, J. Therm. Anal. Calorim. 137 (2019) 543–553.
[8] E.M. Materón, A. Wong, T.A. Freitas, et al., A sensitive electrochemical detection of metronidazole in synthetic serum and urine samples using low-cost screen-printed electrodes modified with reduced graphene oxide and C60, J. Pharm. Anal. 11 (2021) 646–652.
[9] A. Awad, F. Fina, A. Goyanes, et al., Advances in powder bed fusion 3D printing in drug delivery and healthcare, Adv. Drug Deliv. Rev. 174 (2021) 406–424.
[10] M.D. Sarker, S. Naghieh, N.K. Sharma, et al., 3D biofabrication of vascular networks for tissue regeneration: A report on recent advances, J. Pharm. Anal. 8 (2018) 277–296.
[11] S.J. Trenfield, A. Awad, C.M. Madla, et al., Shaping the future: recent advances of 3D printing in drug delivery and healthcare, Expert Opin. Drug Deliv. 16 (2019) 1081–1094.
[12] F. Fina, A. Goyanes, M. Rowland, et al., 3D printing of tunable zero-order release printlets, Polymers 12 (2020), 1769.
[13] S. Ayyoubi, J.R. Cerda, R. Fernández-García, et al., 3D printed spherical mini-tablets: Geometry versus composition effects in controlling dissolution from personalised solid dosage forms, Int. J. Pharm. 597 (2021), 120336.
[14] V.M. Vaz, L. Kumar, 3D printing as a promising tool in personalized medicine, AAPS PharmSciTech 22 (2021), 49.
[15] M. Cunha-Filho, M.R. Araújo, G.M. Gelfuso, et al., FDM 3D printing of modified drug-delivery systems using hot melt extrusion: A new approach for individualized therapy, Ther. Deliv. 8 (2017) 957–966.
[16] H. Öblom, J.X. Zhang, M. Pimparade, et al., 3D-printed isoniazid tablets for the treatment and prevention of tuberculosis-personalized dosing and drug release, AAPS PharmSciTech 20 (2019), 52.
[17] F.Q. Pires, I. Alves-Silva, L.A.G. Pinho, et al., Predictive models of FDM 3D printing using experimental design based on pharmaceutical requirements for tablet production, Int. J. Pharm. 588 (2020), 119728.
[18] A. Goyanes, A.B. Buanz, G.B. Hatton, et al., 3D printing of modified-release aminosalicylate (4-ASA and 5-ASA) tablets, Eur. J. Pharm. Biopharm. 89 (2015) 157–162.
[19] K. Ilyés, N.K. Kovács, A. Balogh, et al., The applicability of pharmaceutical polymeric blends for the fused deposition modelling (FDM) 3D technique: Material considerations-printability-process modulation, with consecutive effects on *in vitro* release, stability and degradation, Eur. J. Pharm. Sci. 129 (2019) 110–123.
[20] A. Goyanes, H. Chang, D. Sedough, et al., Fabrication of controlled-release budesonide tablets via desktop (FDM) 3D printing, Int. J. Pharm. 496 (2015) 414–420.
[21] W. Kempin, V. Domsta, I. Brecht, et al., Development of a dual extrusion printing technique for an acid- and thermo-labile drug, Eur. J. Pharm. Sci. 123 (2018) 191–198.
[22] I. El Aita, J. Breitkreutz, J. Quodbach, On-demand manufacturing of immediate release levetiracetam tablets using pressure-assisted microsyringe printing, Eur. J. Pharm. Biopharm. 134 (2019) 29–36.
[23] G. Matijašić, M. Gretić, J. Vinčić, et al., Design and 3D printing of multicompartmental PVA capsules for drug delivery, J. Drug Deliv. Sci. Technol. 52 (2019) 677–686.
[24] A.Q. Low, J. Parmentier, Y.M. Khong, et al., Effect of type and ratio of solubilising polymer on characteristics of hot-melt extruded orodispersible films, Int. J. Pharm. 455 (2013) 138–147.
[25] M. Sadia, B. Arafat, W. Ahmed, et al., Channelled tablets: An innovative approach to accelerating drug release from 3D printed tablets, J. Contr. Release 269 (2018) 355–363.
[26] F. Dores, M. Kuźmińska, C. Soares, et al., Temperature and solvent facilitated extrusion based 3D printing for pharmaceuticals, Eur. J. Pharm. Sci. 152 (2020), 105430.
[27] J.X. Zhang, X. Feng, H. Patil, et al., Coupling 3D printing with hot-melt extrusion to produce controlled-release tablets, Int. J. Pharm. 519 (2017) 186–197.
[28] T.C. Okwuosa, C. Soares, V. Gollwitzer, et al., On demand manufacturing of patient-specific liquid capsules via co-ordinated 3D printing and liquid dispensing, Eur. J. Pharm. Sci. 118 (2018) 134–143.
[29] A. Melocchi, G. Loreti, M.D. Del Curto, et al., Evaluation of hot-melt extrusion and injection molding for continuous manufacturing of immediate-release tablets, J. Pharm. Sci. 104 (2015) 1971–1980.
[30] D.M. Smith, Y. Kapoor, G.R. Klinzing, et al., Pharmaceutical 3D printing: Design and qualification of a single step print and fill capsule, Int. J. Pharm. 544 (2018) 21–30.
[31] L.F.B. Malaquias, H.L. Schulte, J.A. Chaker, et al., Hot melt extrudates formulated using design space: One simple process for both palatability and dissolution rate improvement, J. Pharm. Sci. 107 (2018) 286–296.
[32] G. Kollamaram, D.M. Croker, G.M. Walker, et al., Low temperature fused deposition modeling (FDM) 3D printing of thermolabile drugs, Int. J. Pharm. 545 (2018) 144–152.
[33] K. Klímová, J. Leitner, DSC study and phase diagrams calculation of binary systems of paracetamol, Thermochim. Acta 550 (2012) 59–64.
[34] A.L. Lima, L.A.G. Pinho, J.A. Chaker, et al., Hot-melt extrusion as an advantageous technology to obtain effervescent drug products, Pharmaceutics 12 (2020), 779.
[35] E. Villicaña-Molina, E. Pacheco-Contreras, E.A. Aguilar-Reyes, et al., Pectin and chitosan microsphere preparation via a water/oil emulsion and solvent evaporation method for drug delivery, Int. J. Polym. Mater. Polym. Biomater. 69 (2020) 467–475.
[36] M.D. Phale, P.D. Hamrapurkar, Optimization and establishment of a validated stability-indicating HPLC method for study of the stress degradation behavior of metoprolol succinate, J. AOAC Int. 93 (2010) 911–916.
[37] B. Marciniec, M. Ogrodowczyk, B. Czajka, et al., The influence of radiation sterilisation on some β-blockers in the solid state, Thermochim. Acta 514 (2011) 10–15.
[38] R.M. Borkar, B. Raju, R. Srinivas, et al., Identification and characterization of stressed degradation products of metoprolol using LC/Q-TOF-ESI-MS/MS and $MS^n$ experiments, Biomed. Chromatogr. 26 (2012) 720–736.
[39] Y. Ikeuchi-Takahashi, S. Ito, A. Itokawa, et al., Preparation and evaluation of orally disintegrating tablets containing taste masked microparticles of acetaminophen, Pharmazie 75 (2020) 2–6.
[40] M.A. Alhnan, A.W. Basit, In-process crystallization of acidic drugs in acrylic microparticle systems: Influence of physical factors and drug-polymer interactions, J. Pharm. Sci. 100 (2011) 3284–3293.
[41] R. Pezzoli, J.G. Lyons, N. Gately, et al., Stability studies of hot-melt extruded ternary solid dispersions of poorly-water soluble indomethacin with poly(-vinyl pyrrolidone-*co*-vinyl acetate) and polyethylene oxide, J. Drug Deliv. Sci. Technol. 52 (2019) 248–254.
[42] G.G.G. de Oliveira, A. Feitosa, K. Loureiro, et al., Compatibility study of paracetamol, chlorpheniramine maleate and phenylephrine hydrochloride in physical mixtures, Saudi Pharm. J. 25 (2017) 99–103.
[43] G. Verstraete, W. De Jaeghere, J. Vercruysse, et al., The use of partially hydrolysed polyvinyl alcohol for the production of high drug-loaded sustained release pellets via extrusion-spheronisation and coating: *In vitro* and *in vivo* evaluation, Int. J. Pharm. 517 (2017) 88–95.

[44] K.L. O'Donnell, G.S. Oporto-Velásquez, N. Comolli, Evaluation of acetaminophen release from biodegradable poly (vinyl alcohol) (PVA) and nanocellulose films using a multiphase release mechanism, Nanomaterials 10 (2020), 301.
[45] M.K. Lai, R.C-C. Tsiang, Encapsulating acetaminophen into poly(L-lactide) microcapsules by solvent-evaporation technique in an O/W emulsion, J. Microencapsul. 21 (2004) 307–316.
[46] Y.S. Yang, A. Gupta, A.S. Carlin, et al., Comparative stability of repackaged metoprolol tartrate tablets, Int. J. Pharm. 385 (2010) 92–97.
[47] J. Varshosaz, H. Faghihian, K. Rastgoo, Preparation and characterization of metoprolol controlled-release solid dispersions, Drug Deliv. 13 (2006) 295–302.
[48] K.P. Sawant, R. Fule, M. Maniruzzaman, et al., Extended release delivery system of metoprolol succinate using hot-melt extrusion: Effect of release modifier on methacrylic acid copolymer, Drug Deliv. Transl. Res. 8 (2018) 1679–1693.
[49] S.M. Alshahrani, W. Lu, J.B. Park, et al., Stability-enhanced hot-melt extruded amorphous solid dispersions via combinations of Soluplus® and HPMCAS-HF, AAPS PharmSciTech 16 (2015) 824–834.
[50] A.B. Albadarin, C.B. Potter, M.T. Davis, et al., Development of stability-enhanced ternary solid dispersions via combinations of HPMCP and Soluplus® processed by hot melt extrusion, Int. J. Pharm. 532 (2017) 603–611.